Relevance of chaos in numerical solutions of quantum billiards

Baowen Li,[1,2] Marko Robnik,[2] and Bambi Hu[1,3]
[1]*Department of Physics and Centre for Nonlinear Studies, Hong Kong Baptist University, Hong Kong, China*
[2]*Center for Applied Mathematics and Theoretical Physics, University of Maribor, Maribor, Slovenia*
[3]*Department of Physics, University of Houston, Houston, Texas 77204*
(Received 29 July 1997; revised manuscript received 5 November 1997)

In this paper we have tested several general numerical methods in solving the quantum billiards, such as the boundary integral method (BIM) and the plane-wave decomposition method (PWDM). We performed extensive numerical investigations of these two methods in a variety of quantum billiards: integrable systems (circles, rectangles, and segments of a circular annulus), Kolmogorov-Arnold-Moser systems (Robnik billiards), and fully chaotic systems (ergodic, such as a Bunimovich stadium, Sinai billiard, and cardiod billiard). We have analyzed the scaling of the average absolute value of the systematic error ΔE of the eigenenergy in units of the mean level spacing with the density of discretization b (which is the number of numerical nodes on the boundary within one de Broglie wavelength) and its relationship with the geometry and the classical dynamics. In contradistinction to the BIM, we find that in the PWDM the classical chaos is definitely relevant for the numerical accuracy at a fixed density of discretization b. We present evidence that it is not only the ergodicity that matters, but also the Lyapunov exponents and Kolmogorov entropy. We believe that this phenomenon is one manifestation of quantum chaos. [S0163-1829(98)05604-5]

PACS number(s): 05.45.+b, 02.70.Rw, 03.65.Ge

I. INTRODUCTION

It is quite embarrassing to realize that in an attempt to numerically solve the Helmholtz equation

$$\nabla_{\mathbf{r}}^2\psi(\mathbf{r})+k^2\psi(\mathbf{r})=0, \tag{1}$$

satisfied by the scalar solution $\psi(\mathbf{r})$ with eigenenergy $E=k^2$ inside a connected plane domain $\mathcal{B}$ with the Dirichlet boundary condition $\psi(\mathbf{r})=0$ on the boundary $\partial\mathcal{B}$, one can face enormous difficulties in cases of ''problematic'' geometries such as various nonconvex shapes. This is precisely the problem of solving and describing the quantum billiard $\mathcal{B}$ as a Hamiltonian dynamical system, which is thus just the two-dimensional Schrödinger problem for a free point particle moving inside the enclosure $\partial\mathcal{B}$, described by the wave function $\psi(\mathbf{r})$ with the eigenenergy $E=k^2$. The corresponding classical problem is the classical dynamics of a freely moving point particle obeying the law of specular reflection upon hitting the boundary $\partial\mathcal{B}$. Quantum billiards and their correspondence to their classical counterparts, especially in the semiclassical level, are important model systems in studies of quantum chaos [1–3]. There are several *general* methods for a numerical solution of Eq. (1) such as the boundary integral method (BIM) (see, e.g., [4–6]) and the plane-wave decomposition method (PWDM), introduced and advocated by Heller [7], whose analysis, especially in the light of the relevance of classical chaos, is the subject of our present paper. Another quite general method is the conformal mapping diagonalization technique introduced by Robnik [8] and further developed by Berry and Robnik [9], Prosen and Robnik [10], and Bohigas *et al.* [11], which in principle should work for any shape, whereas, in practice, it is used for shapes for which the conformal mapping onto the unit disk (or some other integrable geometries admitting a simple basis for the representation) is sufficiently simple (possibly also analytic). These methods can face quite similar problems in cases of almost intractable geometries, but they are to some extent complementary. For example, the conformal mapping diagonalization technique can provide a complete set of all eigenenergies up to some maximal value beyond which the calculations cannot be performed due to the lack of computer storage random access memory, which means that we cannot reach very high-lying eigenstates. (Our present record [10] is about 35 000 for the size of the banded matrix that we diagonalize in double precision, yielding at least 12 000 good levels with accuracy of at least 1% of the mean level spacing.)

However, using the PWDM it is possible to go higher in energy by orders of magnitude, but then only a few selected states can be calculated with many intermediate states in the spectral stretch missing. Therefore, the geometry of some interesting and representative high-lying states can be analyzed, but the sample is typically not sufficiently complete (there are many states missing) to perform statistical analysis. (See, e.g., our recent papers on this topic [12,13].) The reasons for a failure of one of these methods can be quite different. For example, in the BIM the main difficulty stems from the existence of ''exterior chords'' in nonconvex geometries in its standard formulation (see Sec. III), but the trouble might be overcome by an appropriate reformulation of the method adapted to the correct semiclassical behavior. We will discuss this in Sec. III, where we also show that classical chaos is completely irrelevant for the BIM. On the contrary, in the PWDM we find that the classical chaos is relevant for numerical accuracy especially in the semiclassical limit of the sufficiently small effective Planck constant $\hbar_{eff}$ reached at sufficiently high eigenenergies. This demonstration and its qualitative explanation is the main subject of our present paper. To give a specific example we should mention isospectral billiards discovered and proved by Gordon *et al.* [14], which have been investigated experimentally

by Sridhar and Kudrolli [15] and it is also our experience [16] that the BIM fails in this case (namely, due to strong nonconvexities), whereas the PWDM at $b=12$ yields the accuracy of eigenenergies of within a few percent of the mean level spacing, except for some very special eigenmodes for which surprisingly we find agreement within double precision (16 digits) and which are characterized by the fact that these eigenvalues agree with the analytic solutions for the triangles within single precision (eight digits). So the fact that in this and similar cases the experimental precision (for some levels) exceeds the best possible numerical precision even when using the best available methods is embarrassing for a theoretician, but also motivation for further work.

The paper is organized as follows. In Sec. II we focus our attention on the PWDM. In Sec. III we first point out some serious flaws in the derivation of the BIM in the literature and show how the final formula (which nevertheless was correct) should be derived in a *regularized* way and then discuss the numerical results of the BIM and the relevance with classical dynamicss and geometry, etc. In Sec. IV we give a discussion and conclusions.

II. THE PLANE-WAVE DECOMPOSITION METHOD OF HELLER

A. The numerical procedure of the PWDM

In this section we present our general exposition of the PWDM following [12]. To solve the Schrödinger equation (1) for $\psi(\mathbf{r})$ with the Dirichlet boundary condition $\psi(\mathbf{r})=0$ on $\partial\mathcal{B}$ we use the ansatz of the superposition of plane waves (originally due to Heller [7])

$$\psi(\mathbf{r})=\sum_{j=1}^{N} a_j \cos(k_{xj}x+k_{yj}y+\phi_j), \tag{2}$$

where $k_{xj}=k\cos\theta_j$, $k_{yj}=k\sin\theta_j$, $k^2=E$, and we use the notation $\mathbf{r}=(x,y)$. N is the number of plane waves and ϕ_j are *random phases*, drawn from the interval $[0,2\pi)$, assuming a uniform distribution, and $\theta_j=2j\pi/N$ determining the direction angles of the wave vectors chosen equidistantly. The ansatz (2) solves the Schrödinger equation (1) in the interior of the billiard region $\mathcal{B}$, so that we have only to satisfy the Dirichlet boundary condition. Taking the random phases, as we discovered, is equivalent to spreading the origins of plane waves all over the billiard region, and at the same time this results in reducing the CPU time by almost a factor of 10. For a given k we set the wave function equal to zero at a finite number M of boundary points (primary nodes) and equal to 1 at an arbitrarily chosen interior point. Of course, $M\geqslant N$. This gives an inhomogeneous set of equations that can be solved by matrix inversion. Usually the matrix is very singular and thus the *singular value decomposition* method has been invoked [7,17]. After obtaining the coefficients a_j we calculate the wave functions at other boundary points (secondary nodes). We always have three secondary nodes between a pair of primary nodes. The experience shows that a further increase of the number of secondary nodes does not enhance the accuracy. The sum of the squares of the wave function at all the secondary nodes (Heller called this sum ''tension'') would be ideally zero if k^2 is an eigenvalue and if Eq. (2) is the corresponding exact solution of Eq. (1). In practice it is a positive number. Therefore, the eigenvalue problem now is to find the minimum of the tension. In our numerical procedure we have looked for the zeros of the first derivative of the tension; namely, the derivative is available analytically or explicitly from Eq. (2) once the amplitudes a_j have been found. In this paper we make the choice $M=N$ since it proved to be sufficient for calculating the lowest 100 states whose accuracy we analyze. (For the high-lying states studied in our paper [12], we have used $M=5N/3$.) It must be pointed out that the wave functions obtained in this way are not (yet) normalized due to the arbitrary choice of the interior point where the value of the wave function has been arbitrarily set equal to unity. We therefore explicitly normalize these wave functions before embarking on the analysis of their properties.

The accuracy of this method of course depends on the number of plane waves (N) and on the number of the primary nodes (M) and we have a considerable freedom in choosing N and $M\geqslant N$. In order to reach a sufficient accuracy the experience shows that we should take at least $N=3\mathcal{L}/\lambda_{de\ Broglie}$ and $M=N$, where $\mathcal{L}$ is the perimeter of the billiard and $\lambda_{de\ Broglie}$ is the de Broglie wavelength, equal to $2\pi/k$. With this choice in the present context and for the lowest 100 states we reach the double precision accuracy (16 digits) for all levels of integrable systems such as the rectangular billiard (where the eigenenergies can be given trivially analytically) and the circular billiard, but also for the Robnik billiard $\mathcal{B}_\lambda$ for small $\lambda\leqslant 0.1$. Introducing the density of discretization b defined as the number of numerical nodes per one de Broglie wavelength on the boundary, we thus write the number of plane waves $N=b\mathcal{L}/\lambda_{de\ Broglie}=b2\pi\mathcal{L}/k$.

The main problem of investigation in this paper is to study the dependence of the systematical numerical error ΔE (i.e. the error due to the finite discretization) on the density of discretization b and the dependence of ΔE on the geometry (billiard shape parameter) at fixed b. In order to perform a systematic analysis the errors should be measured in some natural units and in our case this is of course just the mean level spacing, which, according to the leading term of the Weyl formula, is equal to $4\pi/\mathcal{A}$, where $\mathcal{A}$ is the area of the billiard $\mathcal{B}$. From now on we shall always assume that ΔE of a particular energy level is in fact measured in such natural units. Of course one immediately realizes that the error ΔE fluctuates wildly from state to state (see Figs. 5 and 7) so that generally nothing can be predicted about it individually. Therefore, the approach must be a statistical one and so we typically take an average of the errors ΔE over a suitable ensemble of states. Specifically, in all cases of this paper we have taken the average of the absolute values of ΔE over the lowest 100 states (of a given symmetry class) and denoted it by $\langle|\Delta E|\rangle$. It is important and should be mentioned that we have also checked the stationarity of such an average value over consecutive spectral stretches of 100 states each, so that our procedure does make sense. In addition, we have also investigated the standard deviation $\sigma_{|\Delta E|}=\langle(|\Delta E|-\langle|\Delta E|\rangle)^2\rangle^{1/2}$, which always has the same order of magnitude as the average value.

It turns out that the accuracy of energy levels depends nontrivially on b, unlike in the BIM, where we find always a

power law (see Sec. III), namely, it typically shows broken power law. By this we mean that $\langle|\Delta E|\rangle$ obeys a power law

$$\langle|\Delta E|\rangle = Ab^{-\alpha}, \tag{3}$$

with very large α for sufficiently small b, $b \leqslant b_c$, whereas for larger $b \geqslant b_c$ it obeys a rather flat power law with very small positive α (close to zero). Therefore in contradistinction to the BIM, it is difficult to explore the general dependence of $\langle|\Delta E|\rangle$ on b if there is any such universality at all. However, in order to investigate the dependence of the accuracy on geometry and the implied dynamical properties of billiards, we have decided to fix the value of b and have chosen $b=12$, and then we look at the dependence of $\langle|\Delta E|\rangle$ on the shape parameters of three one-parameter billiards, namely, the Robnik billiard, the Bunimovich stadium, and the Sinai billiard.

Finally, we would like to discuss how to estimate the error. As usual, to speak of an error we need to have a standard value. The question is how to get the standard values in different quantum billiards. As for the integrable billiard, such as a rectangle, we know analytically the exact values. For a circular billiard, they are the zeros of the Bessel function, which can be calculated very precisely. However, for other billiards, in particular the chaotic billiards, there are no true, accurate values available (otherwise we do not need the numerical methods anymore). In fact, both the PWDM and BIM can be self-tested for their accuracy. On the one hand, in both cases, the numerical value at very large b can be regarded as the ''true'' value. On the other hand, in the PWDM one may change the position of the interior point and compare the two lists of eigenenergies obtained. Moreover, since we have also some other special methods invented for the billiard of a specific geometry, such as the diagonalization method for the Robnik billiard and the scattering approach for the Sinai billiard, in these techniques the accuracy is well controlled and we may obtain more accurate results than the BIM and PWDM; thus we can use the eigenenergy list from them as the standard value.

In our studies in this paper, the ''standard values'' of the Robnik billiard are provided by Prosen [18] by using the diagonalization method with a very large dimension of the matrix and thus the lowest 1000 eigenvalues are guaranteed with an accuracy of at least 10^{-12} in units of the mean level spacing for the large shape parameter λ. The eigenvalues of the Sinai billiard were provided by Schanz and Smilansky [19] by using their scattering method. The accuracy is about 10^{-7} of the mean level spacing, which is already high enough for our purpose. For the billiards whose eigenvalues are not available from other methods, we always take the eigenvalues at very large density of discretization b (say 30) as the true value.

B. Relevance of chaos with the numerical accuracy

As is well known, in the classically integrable quantum Hamiltonian systems in the semiclassical limit (of sufficiently small $\hbar$) the eigenfunction can locally be described by a *finite* superposition of plane waves with the same wave number; in the case of plane billiards it is $k=\sqrt{E}$. If the quantum system has ergodic classical dynamics then in the semiclassical limit locally the wave function can be represented as a superposition of *infinitely* many plane waves with the same k and with the wave vectors being isotropically distributed on the circle of radius k [20]. Moreover, the ergodicity suggests random phases for the ensemble of plane waves, which implies that to the lowest approximation the wave function is a Gaussian random function. While this is a good starting approximation, originally due to Berry [20] and recently verified by Aurich and Steiner [21] and also by Li and Robnik [12], the phases are actually not random but correlated in a subtle way dictated by the classical dynamics, especially along the short and the least unstable periodic orbits, which is the origin of the scar phenomenon [7,22–25]. Thus we can qualitatively very well understand that the PWDM should work well or even brilliantly in cases of classically integrable billiards, whereas in the ergodic systems we expect a severe degradation of the accuracy (at fixed b) simply because the finite number of plane waves cannot capture the correct (infinite) superposition of plane waves everywhere in the interior of the billiard. If the system is a generic system of a mixed type with regular and irregular regions coexisting in the classical phase space, a scenario described by the Kolmogorov-Arnold-Moser (KAM) theory, then the degradation of accuracy (at fixed b) with increasing fractional measure of the chaotic component (denoted by ρ_2) is certainly expected. However, ρ_2 is not the only parameter that controls the accuracy (at fixed b) since, as we shall see, the dynamical properties such as the diffusion time, Lyapunov exponent, and Kolmogorov entropy also play a role. It is the aim of the present paper to numerically explore this type of behavior in three different billiard systems.

The first billiard system is defined as the quadratic (complex) conformal map $w=z+\lambda z^2$ from the unit disk $|z|\leqslant 1$ from the z plane onto the $w=(x,y)$ complex plane. The system has been introduced by Robnik [26] and further studied by Hayli *et al.* [27], Frisk [28], and Bruus and Stone [29] for various parameter values λ. Since the billiard (usually called the Robnik billiard by the people in the community) has an analytic boundary it goes continuously from the integrable case (circle, $\lambda=0$) through a KAM-like regime of small $\lambda \leqslant 1/4$ with mixed classical dynamics and becomes nonconvex at $\lambda=1/4$ (the bounce map becomes discontinuous), where the Lazutkin caustics (invariant tori) are destroyed, giving way to ergodicity. It was shown by Robnik [26] that the classical dynamics at these values of λ is predominantly chaotic (almost ergodic), although Hayli *et al.* [27] have shown that there are still some stable periodic orbits surrounded by very tiny stability islands up to $\lambda=0.2791$. At larger λ we have reason and numerical evidence [30] to expect that the dynamics can be ergodic. Recently it has been proven rigorously by Markarian [31] that for $\lambda=1/2$ (a cardioid billiard) the system is indeed ergodic, mixing, and K. This was further motivation to study the cardioid billiard classically, semiclassically, and quantitatively by several groups, e.g., Bäcker *et al.* [32] and Bruus and Whelan [33]. The billiard shape for $\lambda=0.4$ is shown (the upper half) in Fig. 1(a). Since all states are either even or odd we can take into account these symmetry properties explicitly. In fact, we want to specialize to the odd eigenstates only. Therefore, in order to *a priori* satisfy the Dirichlet boundary condition on the abscissa of Fig. 1(a) we specialize the general ansatz (2) to the form

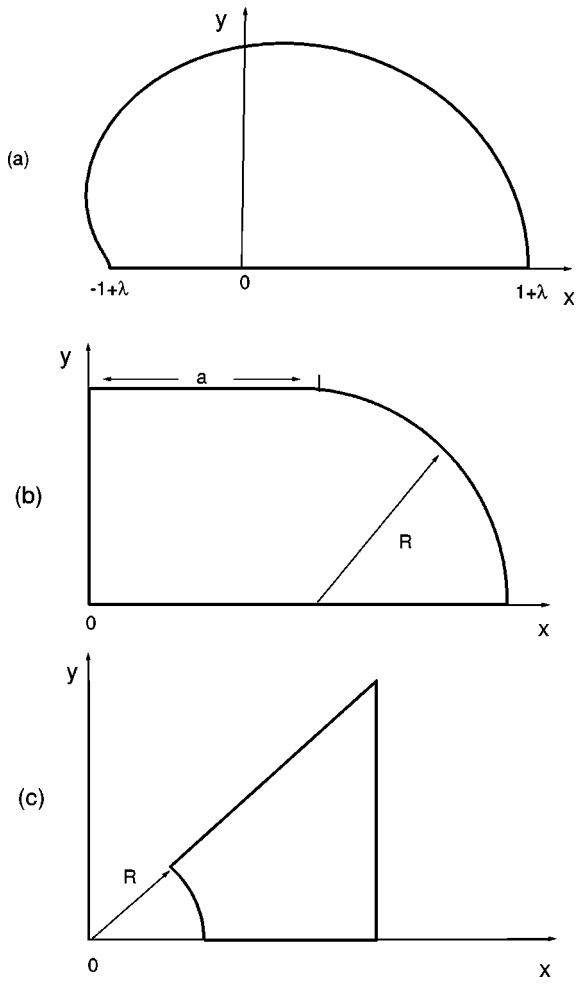

FIG. 1. Geometry of the boundary of the three desymmetrized billiards: (a) the Robnik billiard, (b) the Bunimovich stadium, (c) and the Sinai billiard.

$$\psi(\mathbf{r}) = \sum_{j=1}^{N} a_j \cos(k_{xj}x + \phi_j)\sin(k_{yj}y), \tag{4}$$

where all the quantities are precisely as in Eq. (2) except that the N discretization (primary) nodes are equidistantly located only along the half of the full billiard boundary, so that b is exactly the same as in using the ansatz (2) for the full billiard.

In Fig. 2 we show the results for this billiard, namely, we plot $\langle|\Delta E|\rangle$ (in logarithmic units) versus λ at fixed $b=12$. Close to integrability ($\lambda \leqslant 0.1$) we reach the accuracy within 14–15 digits, which is almost the double precision on our machine (16 digits), in which all our calculations have been performed. As the value of λ increases we observe a dramatic deterioration of the accuracy where $\langle|\Delta E|\rangle$ increases by many orders of magnitude, namely, by almost 13 decades, leveling off at $\langle|\Delta E|\rangle$ approximately equal to 10^{-2}, which means that we have now the accuracy of only a few percent of the mean level spacing. This dramatic but quite smooth increase of $\langle|\Delta E|\rangle$ is certainly related to the emergence of classical chaos with increasing λ, but definitely is *not* controlled merely by ρ_2 because ρ_2 reaches the value of 1 (almost ergodicity) already at $\lambda = 1/4$ [10,26], whereas $\langle|\Delta E|\rangle$ still varies considerably in the region $\lambda \geqslant 1/4$. Thus it is obvious that in the semiclassical picture also other classical dynamical properties (measures of the ''hardness'' of chaos) play an important role. Although we do not have a quantitative theory yet, one should observe that according to Robnik [26], the Lyapunov exponent and Kolmogorov entropy (h) vary also quite smoothly with λ, suggesting a speculation that there might be a relation between $\langle|\Delta E|\rangle$ and h.

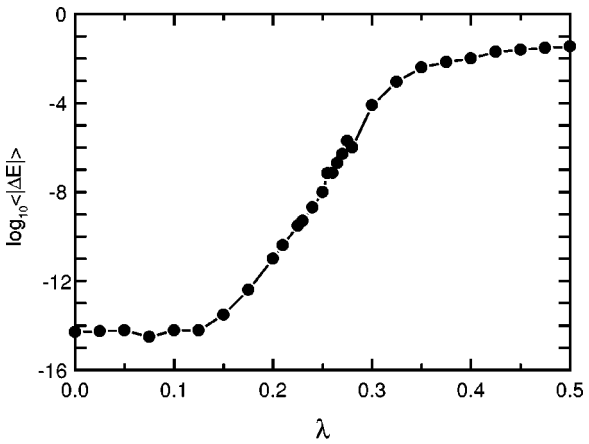

FIG. 2. Ensemble-averaged (over 100 lowest odd eigenstates) absolute error (measured in units of the mean level spacing) $\langle|\Delta E|\rangle$ (in logarithmic units) versus the billiard shape parameter λ for the Robnik billiard with a fixed density of boundary discretization $b=12$. The numerical points are denoted by ●, which are joined by a line to guide the eye.

Another demonstration of the effectivity of the PWDM and its accuracy is displayed in Table I, where we show the numerical value of the scalar product of two consecutive normalized eigenstates, namely, the ground state and the first excited state, denoted by O_{12}, which ideally should be zero. We see here too that the accuracy decreases (by orders of magnitude) sharply but smoothly with increasing shape parameter λ.

It is then interesting to similarly analyze an ergodic system such as the stadium of Bunimovich shown in Fig. 1(b), where the shape parameter is a/R and we have looked at the results for $0 \leqslant a/R \leqslant 10$. In fact, for our purposes we have chosen and fixed $R=1$ in all cases. Since this billiard is known to be rigorously ergodic (and mixing and K) for any $a>0$ in this case ρ_2 is exactly 1 and constant. We have calculated the lowest 100 energy levels of the odd-odd sym-

TABLE I. Test of the orthogonality of the eigenstates and the scalar product of two consecutive normalized wave functions O_{12}, namely, the ground state and the first excited state, for the Robnik billiard at different shape parameters. The number in brackets represents the power of 10.

λ	O_{12}
0	2.0[−16]
0.1	−5.0[−15]
0.2	7.8[−10]
0.3	4.8[−6]
0.4	5.5[−4]
0.5	1.5[−3]

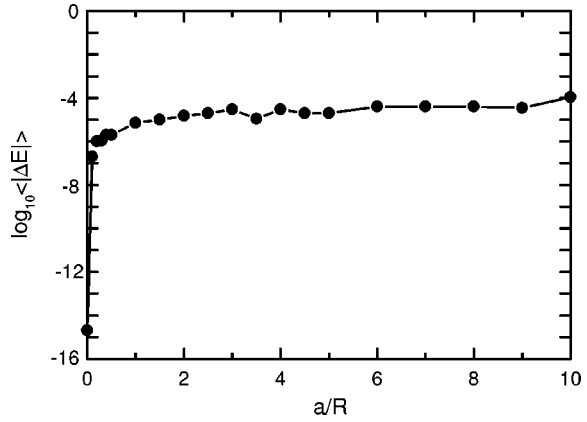

FIG. 3. Ensemble-averaged (over 100 lowest odd-odd eigenstates) absolute error (measured in units of the mean level spacing) (in logarithmic units) versus the billiard shape parameter a/R for the Bunimovich stadium with a fixed density of boundary discretization $b=12$. The numerical points are denoted by ●, which are joined by a line to guide the eye.

metry class. Therefore, in this case the general ansatz (2) can be specialized as

$$\psi(\mathbf{r})=\sum_{j=1}^{N} a_j \sin(k_{xj}x)\sin(k_{yj}y). \tag{5}$$

Here again the discretization (primary) nodes are only on the outer boundary of the stadium with discretization density $b=12$. From our plot in Fig. 3 we see that in the integrable case of the circle ($a=0$) we again reach the accuracy within at least 14 digits, but this brilliant accuracy at fixed $b=12$ deteriorates almost discontinuously upon increasing a and then $\langle|\Delta E|\rangle$ still increases by about two orders of magnitude when a goes from 0.1 to 10. It appears to us that classical chaos is definitely relevant for the accuracy of the method, which might and should be explained by an appropriate theory in the semiclassical level. As an observation we should mention that the Kolmogorov entropy increases sharply with a/R when a/R goes from 0 to about 1, where it

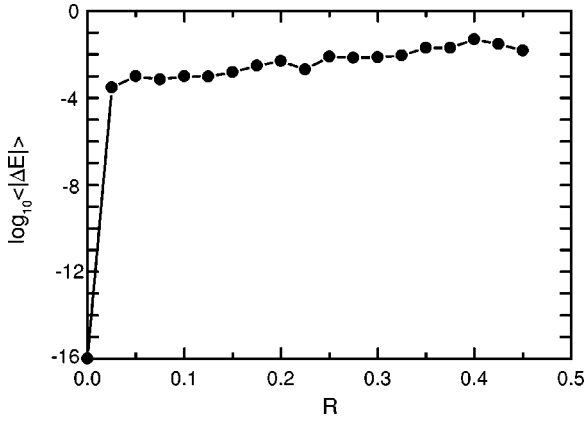

FIG. 4. Ensemble-averaged (over 100 lowest eigenstates) absolute error (measured in units of the mean level spacing) versus the billiard parameter R (the radius of inner circle) for the desymmetrized Sinai billiard with a fixed density of boundary discretization $b=12$. The numerical points are denoted by ●, which are joined by a line to guide the eye.

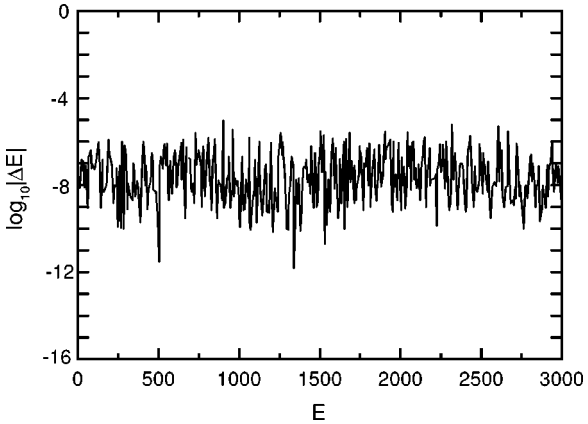

FIG. 5. Absolute error of eigenstates (in logarithmic units) versus eigenenergy for the lowest 400 odd eigenstates of the Robnik billiard at $\lambda=0.27$. The averages over consecutive stretches (of 100 states each) are given in Table II, demonstrating that $\langle|\Delta E|\rangle$ is quite stationary.

reaches the maximum, and then decreases slowly [34], whereas our $\langle|\Delta E|\rangle$ increases monotonically. Thus, if there is a relationship between $\langle|\Delta E|\rangle$ and Kolmogorov entropy it certainly is not a simple one.

We have tested also another system with hard chaos, namely, the Sinai billiard sketched in Fig. 1(c) (desymmetrized). The system is known to be ergodic, mixing, and K. In calculating the 100 lowest energy levels of the desymmetrized Sinai billiard we used the same specialized ansatz as in Eq. (4), thereby taking into account explicitly the Dirichlet boundary condition on the abscissa $y=0$. In this case b is the density of discretization of the equidistant nodes along the rest of the perimeter. Similarly as in the case of the stadium, we easily reach the double precision of 16 digits in the limiting integrable case of zero radius $R=0$, but this accuracy is almost instantly lost by increasing R, as seen in Fig. 4. The value of $\langle|\Delta E|\rangle$ levels off at about 10^{-4}–10^{-2} for all R between 0.025 and 0.45.

As a final technical point we comment on the stationarity of $\langle|\Delta E|\rangle$ as a function of energy, which has been confirmed for the Robnik billiard at $\lambda=0.27$, where the average value over consecutive spectral stretches over 100 states has been found to be quite stable. Specifically, to illustrate this finding we plot in Fig. 5 the absolute values of the errors of the lowest 400 consecutive eigenstates where one can see that the average value over 100 consecutive states is quite stable indeed. This is shown in Table II for four intevals of 100 states each. We should emphasize again that the fluctuation

TABLE II. Stationarity test of $\langle|\Delta E|\rangle$ for the Robnik billiard at $\lambda=0.27$ for the lowest 400 odd eigenstates.

Average stretch	$\langle\|\Delta E\|\rangle$
1–100	1.54[−7]
101–200	2.21[−7]
201–300	2.77[−7]
301–400	2.03[−7]
1–400	2.13[−7]

is very big. We have calculated the standard deviation for these 400 levels; it is $\sigma_{|\Delta E|}=7.40\times10^{-7}$, which has the same order of magnitude as the average value (see Table II). It is our numerical experience that for all cases the standard deviations are always about the same order of average values.

III. BOUNDARY INTEGRAL METHOD

After discussing the PWDM, we now turn to another very important numerical method: the boundary integral method. This method is widely used not only in studying quantum chaos, but also in engineering [35]. In this section we would give an extensive numerical investigation of its accuracy in relation to classical dynamics and geometrical properties. However, before we go into a detailed numerical and technical analysis, we would like to point out two serious flaws in the derivation of the BIM in the literature and show how the final formula, which nevertheless is correct, should be derived in a sound way.

A. A regularized derivation of the BIM

In order to clearly expose the difficulties and the errors in the derivation of the BIM offered in the literature, e.g., in Ref. [5], we present our *regularized* derivation, by which we mean that we construct and use a Green function that automatically (by construction) satisfies the Dirichlet boundary condition (vanishes locally on the boundary $\partial\mathcal{B}$ of the billiard domain $\mathcal{B}$), which is achieved by employing the method of images (see, e.g., the article of Balian and Bloch [36] and the references therein). This will enable us to avoid committing two errors, which, however, luckily compensated for each other. *First*, in taking the normal derivatives on the two sides of Eq. (6) in [5], on the right-hand side we must use the value $\psi(\mathbf{r})$, which is the interior solution inside $\mathcal{B}$, rather than $\frac{1}{2}\psi(\mathbf{r})$, which is the value exactly on the boundary, simply because in taking the derivatives we must evaluate the function at two infinitesimally separated points normal to the boundary. *Second*, this error of taking the unjustified factor 1/2 is then exactly compensated for by another error in arriving at Eq. (8) in [5], namely, by interchanging the integration along the boundary $\partial\mathcal{B}$ and the normal differentiation, because due to singularities on the boundary these two operations do not commute.

Now we offer our regularized derivation. We are searching for the solution $\psi(\mathbf{r})$ with eigenenergy $E=k^2$ obeying the Helmholtz equation (1), with the Dirichlet boundary condition $\psi(\mathbf{r})=0$ on the boundary $\mathbf{r}\in\partial\mathcal{B}$. We will transform this Schrödinger equation for our quantum billiard $\mathcal{B}$ into an integral equation by means of the *regularized* Green function $G(\mathbf{r},\mathbf{r}')$, which solves the defining equation

$$\nabla_{\mathbf{r}}^2 G(\mathbf{r},\mathbf{r}')+k^2G(\mathbf{r},\mathbf{r}')=\delta(\mathbf{r}-\mathbf{r}')-\delta(\mathbf{r}-\mathbf{r}'_R), \tag{6}$$

where $\mathbf{r}$ and $\mathbf{r}'$ are in $\mathcal{B}\cup\partial\mathcal{B}$ and $\mathbf{r}'_R$ is the mirror image of $\mathbf{r}'$ with respect to the tangent at the closest-lying point on the boundary (and thus if $\mathbf{r}'$ is sufficiently close to the boundary then $\mathbf{r}'_R$ is outside the billiard $\mathcal{B}$) (see Fig. 6). The solution can easily be found in terms of the free propagator (the free-particle Green function on the full Euclidean plane)

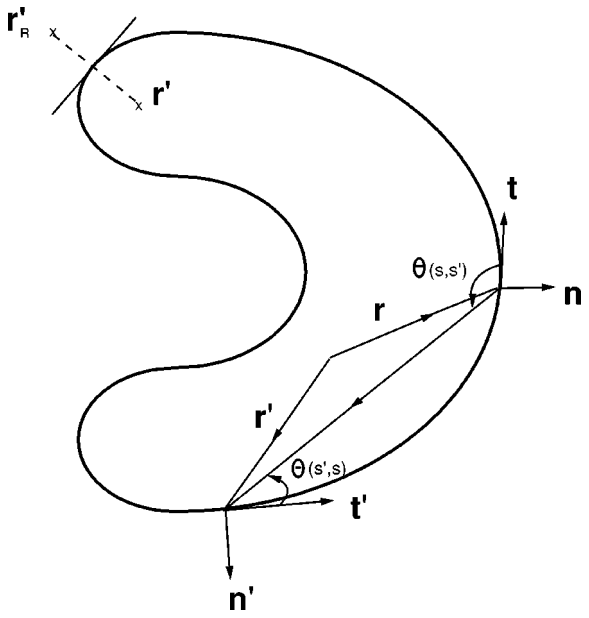

FIG. 6. Notation of the angles and chords used in boundary integral method (BIM).

$$G_0(\mathbf{r},\mathbf{r}')=-\frac{1}{4}iH_0^{(1)}(k|\mathbf{r}-\mathbf{r}'|), \tag{7}$$

where $H_0^{(1)}$ is the zeroth-order Hankel function of the first kind [37], namely,

$$G(\mathbf{r},\mathbf{r}')=G_0(\mathbf{r},\mathbf{r}')-G_0(\mathbf{r},\mathbf{r}'_R), \tag{8}$$

such that now $G(\mathbf{r},\mathbf{r}')$ is zero by construction for any $\mathbf{r}'$ on the boundary $\partial\mathcal{B}$, in contradistinction to the Green's function defined and used in Eq. (5) in [5]. Multiplication of Eq. (6) by $\psi(\mathbf{r})$ and the Helmholtz equation (1) by $G(\mathbf{r},\mathbf{r}')$, subtraction, integration over the area inside $\mathcal{B}$, and using Green's theorem yields

$$\oint ds[\,\psi(\mathbf{r})\mathbf{n}\cdot\nabla_{\mathbf{r}}G(\mathbf{r},\mathbf{r}')-G(\mathbf{r},\mathbf{r}')\mathbf{n}\cdot\nabla_{\mathbf{r}}\psi(\mathbf{r})\,]=\psi(\mathbf{r}'), \tag{9}$$

where s is the arclength on the boundary $\partial\mathcal{B}$ oriented counterclockwise, $\mathbf{n}$ is the unit normal vector to $\partial\mathcal{B}$ at $\mathbf{r}$ oriented outward, and this equation is now valid for *all* $\mathbf{r}'$ inside and on the boundary of $\mathcal{B}$. Since in this equation everything is regular, we can take the normal partial derivatives on both sides. Following the usual notation in [5], we define the normal derivative of ψ at the point s as

$$u(s)=\mathbf{n}\cdot\nabla_{\mathbf{r}}\psi(\mathbf{r}(s)) \tag{10}$$

and thus using the boundary condition $\psi(\mathbf{r})=0$ we arrive at

$$u(s)=-2\oint ds'u(s')\mathbf{n}\cdot\nabla_{\mathbf{r}}G_0(\mathbf{r},\mathbf{r}'). \tag{11}$$

In this way we have correctly derived the main integral equation of the boundary integral method, which is correctly given as Eq. (8) in [5] (where the two errors exactly compensate for each other), so that all the further steps in working out the geometry of Eq. (11) and the numerical discreti-

zations are exactly the same as in [5]. As shown in Fig. 6, we define the length of the chord between two points on the boundary $\mathbf{r}(s)$ and $\mathbf{r}(s')$ as

$$\rho(s,s')=|\mathbf{r}(s)-\mathbf{r}(s')| \tag{12}$$

and the angle $\theta(s',s)$ is the angle between the chord and the tangent to $\partial\mathcal{B}$ at s'. The chord is an oriented separation vector pointing from $\mathbf{r}(s)$ to $\mathbf{r}'=\mathbf{r}(s')$. Of course $\theta(s,s') \neq \theta(s',s)$. Thus following the notation of [5] we can write

$$\mathbf{n}'\cdot\frac{\partial G_0(\mathbf{r},\mathbf{r}')}{\partial\mathbf{r}'}=\sin\theta(s',s)\frac{\partial G_0}{\partial\rho} \tag{13}$$

and we obtain finally

$$u(s)=-\frac{1}{2}ik\oint ds'u(s')\sin\theta(s,s')H_1^{(1)}\{k\rho(s,s')\}. \tag{14}$$

In numerically solving this integral equation we have used precisely the same primitive discretization procedure as in [5], which turned out to be better than some other more sophisticated versions. So we simply divide the perimeter $\mathcal{L}$ into N equally long segments and thus define

$$s_m=m\mathcal{L}/N,\quad \rho(s_l,s_m)=\rho_{lm},$$
$$\theta(s_l,s_m)=\theta_{lm},\quad 1\leqslant l,m\leqslant N. \tag{15}$$

Therefore, numerically, we are searching for the zero of the determinant $\Delta_N(E)=\det(M_{lm})$, where M_{lm} are the matrix elements of the $N\times N$ matrix

$$M_{lm}=\delta_{lm}+\frac{ik\mathcal{L}}{2N}\sin\theta_{lm}H_1^{(1)}(k\rho_{lm}), \tag{16}$$

where $E=k^2$. Due to the asymmetry $\theta_{lm}\neq\theta_{ml}$, this matrix is a general complex non-Hermitian matrix. For the diagonal elements $l=m$, where θ_{lm} is either zero or π, the proper limit of the second term on the right-hand side in Eq. (16) must be taken and then it is equal to $\kappa(s)\mathcal{L}/2\pi N$, where $\kappa(s)$ is the curvature of the boundary at s.

One important aspect of this formalism is the semiclassical limiting form that has been extensively studied by Boasman [6]. At this point we want to make the following comment. In the cases of nonconvex geometries we will have *exterior* chords connecting two points on the boundary such that they lie entirely, or at least partially, outside $\mathcal{B}$. While formally the method and the procedure in such cases is perfectly correct, in reality it might be problematic, which can be seen by considering the semiclassical limit. The formal leading order in the asymptotic expansion of the Hankel function $H_1^{(1)}$ (Debye approximation) does not match the actually correct semiclassical leading approximation that would be spanned by the shortest classical orbit connecting the two points via at least one or many collision points in between. Therefore, we understand and expect that the method must meet some difficulties in cases of nonconvex geometry. This has been partially confirmed in our present work, as we will show in Sec. III B, while the analytical work to reformulate the method including the multiple collision expansions is in progress [38] and is expected to deal satisfactorily with nonconvex geometries.

In the Sec. III B we shall analyze the numerical accuracy of the BIM as a function of the density of discretization

$$b=\frac{2\pi N}{k\mathcal{L}}, \tag{17}$$

in a variety of quantum billiards with integrable, KAM-type, or ergodic classical dynamics, including such with nonconvex geometry. The main result is that there is always a power law so that the error of eigenenergy in units of the mean level spacing, after taking the average of the absolute value over a suitable ensemble of eigenstates, obeys $\langle|\Delta E|\rangle=Ab^{-\alpha}$, but the exponent α (and the prefactor A) is nonuniversal.

B. Numerical results

The numerical procedure we have used to solve the variety of quantum billiards is exactly as described above and therefore it is precisely the same as in [5]. Our main task now is to analyze in detail the behavior of the BIM as a function of the density of discretization b, especially in relation to the geometrical properties of $\mathcal{B}$ (nonconvexities) and in relation to classical dynamics, whose chaotic behavior is expected to imply interesting methodological and algorithmic manifestation of quantum chaos.

Again, like in the PWDM, we have to measure the numerical error of the eigenenergies in units of the mean level spacing and perform some kind of averaging over a suitable ensemble of consecutive states. However, this will make sense only if such a local average of the error is stationary (constant) over a suitable energy interval. This condition has been confirmed to be satisfied in almost all cases that we checked. In the case of the circle billiard and in the case of the cardioid billiard this stationarity of the locally averaged error is shown in Figs. 7(a) and 7(b), respectively, where we plot the data for about 95% of the lowest 1000 odd levels. The average value $\langle|\Delta E|\rangle$ for these two cases are 3.89×10^{-5} (circle) and 1.99×10^{-3} (cardioid billiard), while the standard deviations $\sigma_{|\Delta E|}$ are 3.67×10^{-5} (circle) and 2.91×10^{-3} (cardioid billiard), respectively. Again, like in the case of the PWDM, the standard deviation in the BIM is of the same order as the average value.

We have established that we have always taken the average of the absolute value of the error (in units of the mean level spacing) over a suitable ensemble of eigenstates, for which we have chosen the lowest 100 eigenstates in all cases. Actually, strictly speaking, we have taken about 90–95 levels from the ensemble of the lowest 100 odd levels: Since in using the BIM we always miss some levels, the quota of missing levels typically is a few percent, depending on the step size. In our case the step size is 1/20 of the mean level spacing and the fraction of missing levels varied from about 10% in the integrable billiard with Poisson statistics to about 5% in ergodic cases with Gaussian orthogonal ensemble statistics.

In Figs. 8(a)–8(f) we show the error $\langle|\Delta E|\rangle$ versus b for six billiard shapes. In Fig. 8(a) we have the full circle billiard. In Fig. 8(b) we have a 270° ($=3\pi/2$) segment of the annulus billiard with inner radius $R_1=0.45$ and outer radius

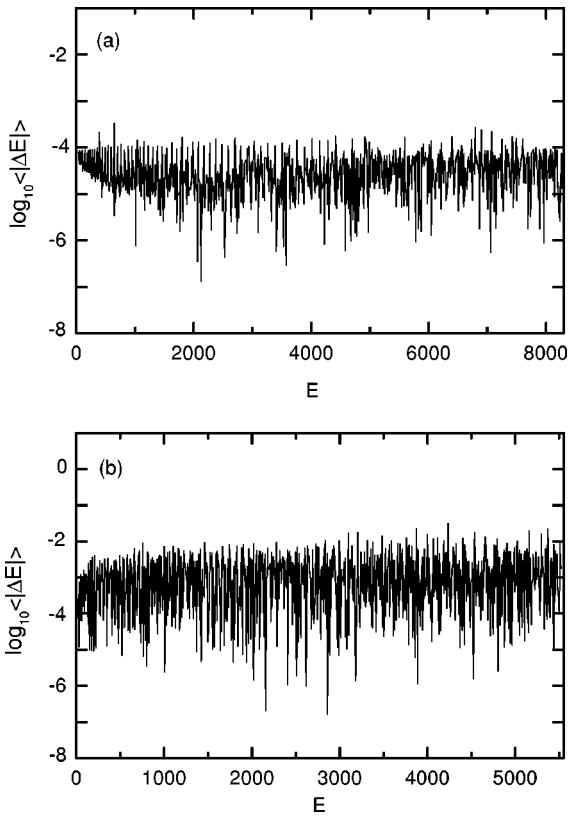

FIG. 7. BIM error (measured in units of the mean level spacing) of eigenstates versus energy. The error is the difference between the BIM value and the exact value. About 95% of the lowest 1000 odd states are shown. Plot (a) is for the full circle billiard and (b) for the cardioid billiard ($\lambda=1/2$). In both cases b is fixed, $b=6$.

$R_2=0.5$. These data were based on the very careful work of Hess [39], who has kindly communicated to us his unpublished results and the analysis, which we have independently checked and confirmed. In Figs. 8(c) and 8(d) we have the Robnik billiard with shape parameters $\lambda=0.15$ and $\lambda=1/2$, respectively. In Fig. 8(e) we show the results for the 1/4 Bunimovich stadium with the size 2×2 for the central square. In Fig. 8(f) we have the 1/4 Sinai billiard with dimensions 2×2 for the square and circular radius $R=1/2$. The best-fitting power-law curve is described by Eq. (3) and is seen to provide a very significant fit in all six cases.

As for the Robnik billiard, one should be reminded that at $\lambda=0$ we have integrable classical dynamics in the circle billiard and at $\lambda=0.15$ we have KAM-type dynamics with islands of stability [16]; it should be emphasized that at $\lambda=1/4$ we have a zero curvature point at $z=-1$ and for all $\lambda>1/4$ the shape is nonconvex) while at $\lambda=1/2$ we have ergodicity and also nonconvex geometry. Technically, in all cases at various λ we have calculated all states by applying the BIM, but then, for technical reasons, compared only the odd states with their exact value, which are supplied by the conformal mapping diagonalization technique [8,10].

In Figs. 8(a)–8(f) we thus observe that there is no clear relationship between the value of α and the degree of classical chaos in all the various billiards. However, it is an interesting ''experimental'' result that the power law (3) seems to be universally valid, with nonuniversal numerical value of α and A.

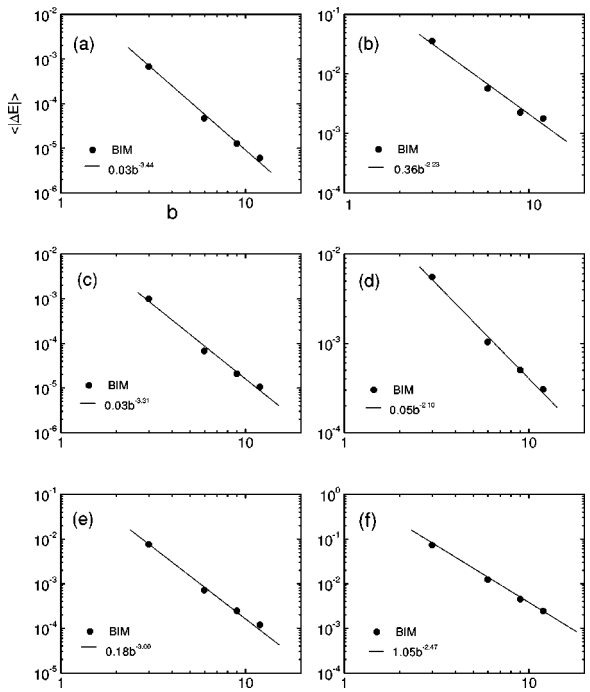

FIG. 8. Ensemble-averaged (over about 95% of the lowest 100 odd eigenstates) absolute BIM error versus the density of boundary discretization b and the best power-law fit for the various billiards. ● represents the numerical data and the curve is the best power-law fit whose α and coefficient A are given in each box. In (a) we have a full circle billiard, in (b) the $3\pi/2$ segment of a circular annulus with inner and outer radii 0.45 and 0.5, respectively, in (c) and (d) the Robnik billiard with $\lambda=0.15$ and $1/2$, respectively, in (e) the 1/4 2×2 Bunimovich stadium, and in (f) the 1/4 Sinai billiard with radius 1/2 inside a square of size 2.

Having established the validity of the power law (3), it is now most interesting and also immensely CPU time consuming (it took almost one month of CPU time on a Convex C3860 to produce Figs. 9 and 10) to look at the variation of α with the billiard shape parameter λ, which is shown in Fig. 9. There is a flat region of almost constant α within $0\leqslant\lambda\leqslant1/4$: It fluctuates slightly around 3.5. At $\lambda>1/4$ the nonconvexities of the boundary appear; unlike naive expec-

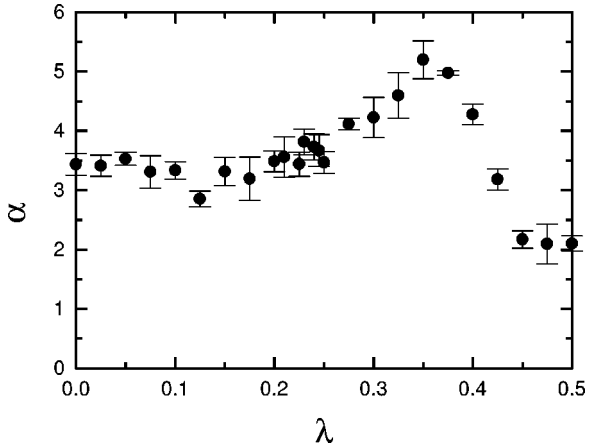

FIG. 9. Power-law exponent α versus the billiard shape parameter λ for the Robnik billiard. The error bars denote the standard deviation from the best fit.

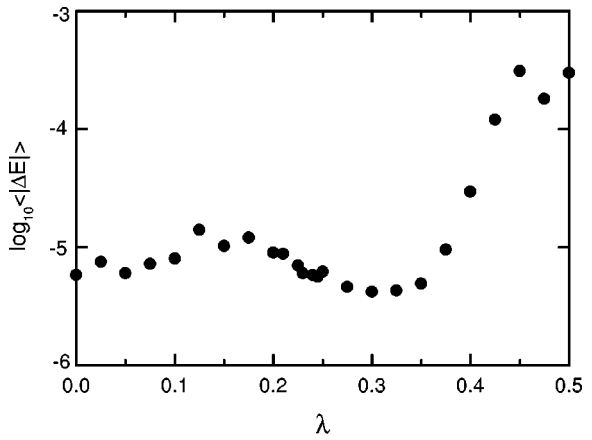

FIG. 10. Ensemble-averaged absolute BIM error (in units of the mean level spacing) $\langle|\Delta E|\rangle$ (in logarithmic units) with fixed $b=12$ against the billiard shape parameter λ for the Robnik billiard.

tation, α now even increases up to a value of slightly larger than 5 reached at $\lambda\approx 0.35$ and then starts to decrease rapidly down to the value of about 2 at $\lambda=1/2$. Therefore, there is no clear correlation with either the nonconvexities or the classical chaos.

In addition to α in Eq. (3) we would also like to know the value of the constant A (the prefactor) in each case. This is given in Fig. 10 by fixing $b=12$ and plotting the mean absolute value of the error (averaged over the lowest 100 odd states) versus λ. Here we see that the mean error $\langle|\Delta E|\rangle$ is almost constant up to $\lambda\leqslant 0.35$ and is equal to about 6×10^{-6}. At $\lambda\geqslant 0.35$ we observe the rapid increasing of $\langle|\Delta E|\rangle$. Here again we cannot draw a clear conclusion, but only note that the error starts to increase rapidly in the regime where classical chaos becomes ''hard'' (the Kolmogorov entropy increases steeply [26]).

Most of our results are summarized in Table III for three classes of billiard systems with different type of classical dynamics, namely, integrable, KAM-type, and ergodic systems. We show the calculated values of α and also the average absolute value of the error $\langle|\Delta E|\rangle$ with fixed value of $b=12$. The table clearly demonstrates that the power law (3) for the BIM is universal, but not the exponent α and the prefactor A. It also demonstrates that classical dynamics has little effect on α, whereas the nonconvexities of the boundary might be more important. There is no theory for α so far except for the circle billiard, for which Boasman [6] predicts $\alpha=3$, which might be marginally compatible with our data. The bizzare behavior of α in various dynamical regimes reminds us of the difficulties in theoretical predictions of, e.g., classical correlation functions [40]. In the table we include also the results of the integrable case of the rectangular equilateral triangle (half of the unit square) where $\alpha=3.28$ is quite large and the ergodic case of the 1/4 Heller's stadium (2×2 square plus two semicircles with a unit radius) in which case $\alpha=3.0$ is also quite large.

TABLE III. Power-law exponent α and the average absolute value of the error $\langle|\Delta E|\rangle$ with $b=12$ for different billiards. For details of the KAM-type billiards see also Figs. 9 and 10.

Type	Quantum billiard	α	$\langle\|\Delta E\|\rangle_{b=12}$
Integrable	circle (half)	2.94 ± 0.17	6.74[−5]
	circle (full)	3.44 ± 0.18	5.97[−6]
	rectangle-triangle	3.28 ± 0.29	4.08[−5]
	segment annulus	2.23 ± 0.24	1.77[−3]
KAM	Robnik (full) $(0<\lambda<1/4)$	≈ 3.4	≈ 5.0[−6]
	Robnik (half) $(0<\lambda<1/4)$	≈ 2.9	≈ 7.0[−5]
Ergodic	stadium (1/4)	3.00 ± 0.16	1.18[−4]
	cardioid (full)	2.10 ± 0.13	3.04[−4]
	Sinai (1/4)	2.47 ± 0.05	3.39[−3]
	Robnik (full) $(0.3<\lambda<1/2)$	see Fig. 9	see Fig. 10

When thinking about improving the efficiency and the accuracy of the BIM we have also tried a more sophisticated version of the BIM, where we have explicitly used a Gaussian integration on the boundary when discretizing our main equation (11). However, this experience has been negative after many careful checks in various billiards and therefore we decided to resort to the primitive discretization of the BIM, which is exactly the same approach as in [5].

IV. DISCUSSION AND CONCLUSIONS

We believe that our present paper presents quite firm numerical (phenomenological) evidence for the relevance of classical chaos for the effectiveness of the PWDM as a quantal numerical method to solve a quantum billiard, which is manifested especially in the semiclassical limit and might and should be explained in terms of an appropriate semiclassical theory. Qualitatively, the reasons for this phenomenon are explained before. The parameter ρ_2, the fractional volume of the chaotic component(s), definitely plays an important role, but is not the only aspect of classical chaos controlling the behavior of the error $\langle|\Delta E|\rangle$ at fixed discretization density b. Namely, even in rigorously ergodic systems where $\rho_2=1$, the error $\langle|\Delta E|\rangle$ might be controlled by the slow diffusion in the classical phase space (diffusive ergodic regime, soft chaos). If the classical diffusion time is much longer than the break time t_{break} ($t_{break}=\hbar/D$, where D is the mean energy level spacing) then the quantal states will be strongly localized in spite of the formal ergodicity (for a demonstration see Ref. [13] for the Robnik billiard and Refs. [41,42] for the stadium billiard) and therefore they mimic a certain amount of regularity, enabling a better accuracy of the PWDM, i.e., $\langle|\Delta E|\rangle$ is smaller than for completely extended chaotic high-lying eigenstates where, according to our experience, somehow $\langle|\Delta E|\rangle$ typically saturates at about a few percent of the mean level spacing, even if we drastically increase b beyond any reasonable limits. Indeed, as can be seen by a comparison of Figs. 2–4, in the case of the stadium this saturation value of $\langle|\Delta E|\rangle$ is about 10^{-4}, which is almost two orders of magnitude smaller than in the Sinai billiard (Fig. 4) and the cardioid billiard (Fig. 2). We think that this is due to the strong localization of eigenstates in the stadium, which is very well known to dis-

play an unusual abundance of scars [7,24,25]. Thus our present work is a motivation for a semiclassical theory to explain this aspect of quantum chaos that exhibits some algorithmic properties of the PWDM in applying it to quantum billiards with a variety of classical dynamics.

Further, we have investigated the behavior of the boundary integral method with respect to the density of discretization b as defined in Eq. (17) (b is the number of numerical nodes per de Broglie wavelength along the boundary) since we expected some relevance of nonconvexities and possibly of classical chaos. In all cases we discovered that there is a power-law behavior described in Eq. (3). We wanted to verify whether there is any systematic effect of classical dynamics of quantum billiards on α and A. The answer is negative. On the other hand, we found that the role of nonconvex geometry of the boundary might be more important, although no final conclusion is possible at this point. The difficulties of the BIM might be expected as explained before, and the easiest way to see that is to consider the semiclassical limiting approximation of the BIM [38]. After explaining two systematic errors in the literature where the integral BIM equation is derived and where luckily the two errors mutually compensate for each other exactly, we have given the correct (*regularized*) derivation and discussed the BIM formalism thus derived. We agree that even in nonconvex geometries it is formally right, but nevertheless practically might be less efficient, which is expected by considering the semiclassical limit mentioned above. Therefore, we suggest a generalization of the BIM by using a multiple reflection (collision) expansion in calculating the most appropriate Green function, which is another subject of our current investigation [38] and is important not only for studies in quantum chaos but also in engineering problems [35] since it would lead to a better efficiency of the BIM, namely, larger α. Most of our results are summarized in Table III, giving the evidence for the above conclusions.

It remains an interesting and important theoretical problem to study the sensitivity of the eigenstates (eigenenergies and wave functions) on the boundary data of eigenfunctions, of which one aspect is also the dependence of the eigenstates on the billiard shape parameter. If such sensitivity correlates with classical chaotic dynamics and at the same time manifests itself in the accuracy of the purely quantal numerical methods, then such a behavior would be one important manifestation of quantum chaos. This interesting line of thought in the search for another aspect of quantum chaos has been further developed in another work [43], where we also present detailed studies of a level curvature distribution and other measures of the sensitivity of the eigenstates.

ACKNOWLEDGMENTS

We thank Dr. Holger Schanz and Professor Uzy Smilansky for the table of the eigenenergies for the Sinai billiard and Dr. Tomaž Prosen for supplying the eigenenergies for the Robnik billiard. We especially thank Dr. Thomas Hesse (University of Ulm) for his results and analysis of the annular billiard and for many useful discussions. We also thank Dr. Vladimir Alkalaj, the director of the National Supercomputer Center, Slovenia, for kind support. The financial support from the Ministry of Science and Technology of the Republic of Slovenia is gratefully acknowledged. This work was supported in part by grants from the Hong Kong Research Grants Council (RGC) and the Hong Kong Baptist University Faculty Research Grant (FRG).

[1] M. C. Gutzwiller, *Chaos in Classical and Quantum Mechanics* (Springer, New York, 1990).
[2] *Chaos and Quantum Systems*, edited by M.-J. Giannoni, A. Voros, and J. Zinn-Justin (Elsevier, Amsterdam, 1991).
[3] G. Casati and B. V. Chirikov, *Quantum Chaos* (Cambridge University Press, Cambridge, 1995).
[4] S. W. McDonald and A. N. Kaufman, Phys. Rev. Lett. **42**, 1189 (1979); Phys. Rev. A **37**, 3067 (1988).
[5] M. V. Berry and M. Wilkinson, Proc. R. Soc. London, Ser. A **392**, 15 (1984).
[6] P. A. Boasman, Nonlinearity **7**, 485 (1994).
[7] E. J. Heller, Phys. Rev. Lett. **53**, 1515 (1984); *Chaos and Quantum Systems* in (Ref. [2]), p. 548.
[8] M. Robnik, J. Phys. A **17**, 1049 (1984).
[9] M. V. Berry and M. Robnik, J. Phys. A **19**, 649 (1986).
[10] T. Prosen and M. Robnik, J. Phys. A **26**, 2371 (1993); **27**, 8059 (1994).
[11] O. Bohigas, D. Boosé, R. Egydio de Carvalho, and V. Marvulle, Nucl. Phys. A **560**, 197 (1993).
[12] B. Li and M. Robnik, J. Phys. A **27**, 5509 (1994).
[13] B. Li and M. Robnik, J. Phys. A **28**, 2799 (1995); **28**, 4843 (1995).
[14] C. Gordon, D. Webb, and S. Wolpert, Bull. Am. Math. Soc. **27**, 134 (1992).
[15] S. Sridhar and A. Kudrolli, Phys. Rev. Lett. **72**, 2175 (1994).
[16] B. Li and M. Robnik (unpublished).
[17] W. H. Press, S. A. Teukolsky, W. T. Vetterling, and B. P. Flannery, *Numerical Recipes* (Cambridge University Press, Cambridge, 1992).
[18] T. Prosen (private communication).
[19] H. Schanz and Uzy Smilansky (private communication); see also H. Schanz and U. Smilansky, Chaos Solitons Fractals **5**, 1289 (1995).
[20] M. V. Berry, J. Phys. A **10**, 2083 (1977).
[21] R. Aurich and F. Steiner, Physica D **64**, 185 (1993).
[22] E. B. Bogomolny, Physica D **31**, 169 (1988).
[23] M. V. Berry, Proc. R. Soc. London, Ser. A **423**, 219 (1989).
[24] B. Li, Phys. Rev. E **55**, 5376 (1997).
[25] B. Li and B. Hu, J. Phys. A **31**, 483 (1998).
[26] M. Robnik, J. Phys. A **16**, 3971 (1983).
[27] A. Hayli, T. Dumont, J. Moulin-Ollagier, and J. M. Strelcyn, J. Phys. A **20**, 3237 (1987).
[28] H. Frisk (unpublished).
[29] A. D. Stone and H. Bruus, Physica B **B189**, 43 (1993); Surf. Sci. **305**, 490 (1993); H. Bruus and A. D. Stone, Phys. Rev. B **50**, 18 275 (1994).
[30] B. Li and M. Robnik (unpublished).
[31] R. Markarian, Nonlinearity **6**, 819 (1993).

[32] A. Bäcker, F. Steiner, and P. Stifter, Phys. Rev. E **51**, 4173 (1995); A. Bäcker, Diplomarbeit, 1995 (unpublished).
[33] H. Bruus and N. D. Whelan, Nonlinearity **9**, 1023 (1996).
[34] G. Benettin and J. M. Strelcyn, Phys. Rev. A **17**, 773 (1978).
[35] P. K. Banerjee, *The Boundary Element Methods in Engineering* (McGraw-Hill, London, 1994).
[36] R. Balian and C. Bloch, Ann. Phys. (N.Y.) **85**, 514 (1974).
[37] *Handbook of Mathematical Functions*, edited by M. Abramowitz and I. A. Stegun (Dover, New York, 1972).
[38] B. Li and M. Robnik (unpublished).
[39] T. Hess (private communication).
[40] P. L. Garrido and G. Gallavotti, J. Stat. Phys. **76**, 549 (1994).
[41] F. Borgonovi, G. Casati, and B. Li, Phys. Rev. Lett. **77**, 4744 (1996).
[42] F. Borgonovi, G. Casati, B. Hu, and B. Li (unpublished).
[43] B. Li and M. Robnik, J. Phys. A **29**, 4387 (1996).